JOURNAL OF CHEMICAL INFORMATION AND MODELING

Article

pubs.acs.org/jcim

Accurate Prediction of Adsorption Energies on Graphene, Using a Dispersion-Corrected Semiempirical Method Including Solvation

Mark A. Vincent and Ian H. Hillier*

School of Chemistry, University of Manchester, Manchester M13 9PL, United Kingdom

ABSTRACT: The accurate prediction of the adsorption energies of unsaturated molecules on graphene in the presence of water is essential for the design of molecules that can modify its properties and that can aid its processability. We here show that a semiempirical MO method corrected for dispersive interactions (PM6-DH2) can predict the adsorption energies of unsaturated hydrocarbons and the effect of substitution on these values to an accuracy comparable to DFT values and in good agreement with the experiment. The adsorption energies of TCNE, TCNQ, and a number of sulfonated pyrenes are also predicted, along with the effect of hydration using the COSMO model.

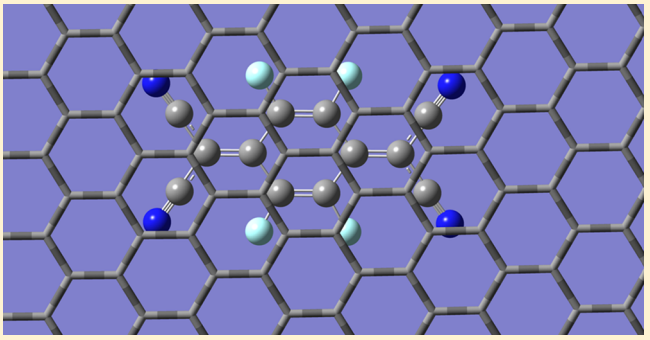

1. INTRODUCTION

Graphene[1,2] has attracted intense interest following the isolation of single-layer graphene (SLG) by mechanical exfoliation and the demonstration of its important properties.[3,4] The processing of graphene is now central to its more widespread use, and activity is focused on finding organic molecules that can exfoliate soluble graphene sheets from graphite.[5−8] A much-used approach is to employ surfactants based upon nanographenes (NGs),[9] which are small polyaromatic hydrocarbons that can effectively bind in a noncovalent manner to the surface of bulk graphite. Such molecules often have, in addition, a hydrophilic group to confer solubility, and hence dispersion, on the graphene-substrate system. Thus, a full study of the noncovalent functionalization of graphene requires an accurate modeling of both $\pi-\pi$ interactions and solvation effects.

Noncovalent interactions of this type are central to many aspects of biochemistry[10] and materials science.[11] The special role of noncovalent $\pi-\pi$ interactions has led to the full range of computational methods being explored to accurately model them. Dispersive forces have been shown to be crucial in these interactions, and although these can be included by both ab initio and density functional theory (DFT) methods, their description using empiric functions as used in traditional force fields has many attractions. Such functions can be readily computed and also parametrized to describe the particular interaction being modeled. Indeed, one of the most successful strategies has been to augment electronic structure schemes with an empiric dispersive term. There have been a number of variants of this approach,[12−17] but the coupling of DFT methods with an atom pairwise C_6R^{-6} potential (DFT-D method) as suggested by Grimme[18] has been successfully applied to a wide range of interactions, particularly those of biological importance.[19] Semiempirical MO methods may also be adapted using a similar strategy to describe noncovalent interactions. Thus, we have developed the dispersion-corrected PM3 method (PM3-D),[20] the necessary adjustment of the PM3 parameters being carried out by fitting to the interaction energies (IE) of a wide number of prototypical biological interactions computed using high level ab initio methods. This resulted in a mean unsigned error in these energies of only a little more than 1 kcal mol^{-1}. More recently the PM6[21,22] and OMx[23] schemes have been corrected in a similar way. The advantage of such semiempirical schemes is that they scale more favorably with the size of the system than do ab initio or DFT methods. Thus, semiempirical methods based upon the neglect of diatomic differential overlap (NDDO), such as AM1, PM3, and PM6, scale as approximately N^3, where N is the number of basis functions, which for these methods employing a minimal basis is proportional to the number of atoms. Hence, these semiempirical methods can be used to study far larger systems than is routinely possible with ab initio or DFT methods without sacrificing the accuracy if properly parametrized.

In this paper, we shall use such a strategy to study the interaction of a range of substrates with graphene. We first describe results for some simple and well-studied aromatic hydrocarbons, followed by a number of substrates that can have a role in the functionalization of graphene. Dispersive-corrected semiempirical methods are ideally suited for these studies because solvation effects can be readily included via well-documented continuum methods.

2. COMPUTATIONAL METHODS AND RESULTS

Although periodic models have been used to study graphene, previous studies have in large measure used small- or medium-

Received: June 25, 2014
Published: August 4, 2014

Table 1. Interaction Energies (kcal mol^{-1}) Computed by DFT and PM6-DH2 Methods for Various Molecules on Models of a Graphene Surface[a]

arene	size	method	E_{ads}	ref
benzene	C110	ωB97X-D/def2-TZVPP	−12.7	27
	C54	ωB97X-D/cc-pVDZ	−13.2	26
	C1006	PM6-DH2	−11.8 [−11.1] (8)	this work
	C574	PM6-DH2	−13.2	this work
	C574	B3LYP-D/TZV2D	−12.7	this work
	C574	M06-2X/6-311G(2d,2p)	−13.1	this work
	C574	M06-2X/TZV2D	−11.0	this work
	C574	ωB97X-D/6-311G(2d,2p)	−12.7	this work
	C574	ωB97X-D/TZV2D	−10.5	this work
	C1006	PM6-DH2	−11.4	26
C6F6	C110	ωB97X-D/def2-TZVPP	−15.5, −15.7	27
	C1006	PM6-DH2	−16.4 [−13.7](8)	this work
naphthalene	C1006	PM6-DH2	−18.9 [-17.4] (7)	this work
	C574	M06-2X/6-311G(2d,2p)	−19.9	this work
	C574	M06-2X/TZV2D	−17.0	this work
	C1006	PM6-DH2	−18.3	26
	C54	ωB97X-D/cc-pVDZ	−21.7	26
	C54	PM6-DH2	−17.5	26
1,5-diaminonaphthalene	C1006	PM6-DH2	−24.1 [−21.1] (6)	this work
pyrene	C1006	PM6-DH2	−29.4 [−26.9] (3)	this work
	periodic	vdW-DF	−25.1	33
nitropyrene	C1006	PM6-DH2	−40.0 [−29.7] (4)	this work
pentacene	C1006	PM6-DH2	−41.0 [−36.8] (5)	this work
TCNE	C1006	PM6-DH2	−15.2 [−13.1] (5)	this work
	C5Ea	BLYP-D3	−22.9	39
	C5Ea	DFTB-D	−14.5	39
TCNQ	C1006	PM6-DH2	−27.2 [−23.2] (6)	this work
	C574	M06-2X/6-311G(2d,2p)	−26.8	this work
	C5Qa	BLYP-D3	−32.2	39
	C5Qa	DFTB-D	−24.3	39
F4-TCNQ	C1006	PM6-DH2	−29.9 [−25.1] (4)	this work

[a]The dispersive and H-bond contributions are given in square brackets. For average values, the number of structures is given in parentheses.

sized finite sheets. We here use the PM6-DH2[22] scheme as implemented in MOPAC.[24] This scheme modifies the PM6 method with corrections for both dispersive and hydrogen-bonding effects, although most of the systems studied here have only dispersive interactions. As implemented, utilizing localized orbitals,[25] PM6-DH2 is particularly appropriate for large systems and has allowed us to optimize structures involving graphene sheets of up to C1006, thus avoiding possible edge effects for large substrates. Semiempirical calculations using graphene sheets of this size have previously been reported[26] but were single-point calculations using geometries optimized at a molecular dynamics level.

2.1. Adsorption of Aromatic Hydrocarbons. Other workers[27] using DFT methods and smaller graphene sheets have found that adsorbates can adopt a number of configurations on the graphene surface, but these structures generally differ in energy by less than 1 kcal mol^{-1} and have correspondingly small barriers connecting them. Thus, the adsorbate is quite mobile on the surface and can adopt a number of configurations at normal temperatures. At the PM6-DH2 level and using a C1006 graphene sheet, we find that the most stable arrangement is when the benzene ring eclipses a similar ring of the graphene, while Wang et al.[27] report structures in which the benzene molecule overlaps more than a single graphene ring. In addition, we have found some eight stationary structures within 1.5 kcal mol^{-1} of our lowest energy structure. Characterization of these structures as minima or transition structures proved problematic, with a number having a small negative harmonic frequency of the order of 10 cm^{-1} including our lowest energy one, which in some cases could well be due to numerical problems in view of the large number of atoms involved. Very high-level electronic structure calculations would be necessary to confidently predict the lowest energy structure, and essentially all calculations employing graphene sheets of a realistic size will yield uncertainties in the interaction energies of at least a few kcal mol^{-1}.

In our comparison of the predictions of DFT and semiempirical calculations, we found it necessary to employ a C574 graphene sheet to render the DFT computations feasible rather than the larger C1006 used for PM6-DH2 calculations. We have considered the adsorption of a number of aromatic hydrocarbons on C574 and have taken a number of structures optimized at the PM6-DH2 level and compared the semi-empirical IE values with those obtained using the B3LYP functional augmented by dispersion terms (B3LYP-D),[28] the M06-2X functional,[29,30] which has been found to successfully describe such noncovalent interactions, and the ωB97X functional corrected for dispersive interactions (ωB97X-D).[31,32] We also compare our calculations with a number of those reported in the literature.[26,27,33] These DFT calculations were carried out using GAUSSIAN 09.[34]

dx.doi.org/10.1021/ci5003729 | J. Chem. Inf. Model. 2014, 54, 2255−2260

We first consider our DFT-based results shown in Table 1. Here, we have used structures for a $C_{574}H_{66}$ sheet optimized at the PM6-DH2 level, which generated ∼14,000 basis functions at the DFT level, rendering geometry optimization to be computationally prohibitive. We have not taken account of BSSE corrections, because following Grimme,[18] we consider the size of both basis sets employed (6-311G (2d, 2p), TZV2D) to be sufficiently large to render these corrections unnecessary. However, we note that other workers[26] report that BSSE corrections reduce the adsorption energy by ∼2 kcal mol^{-1}. We see that for the B3LYP-D method and for both basis sets using the M06-2X functional and the ωB97X-D method, the IE values computed are very close. As far as the actual values are concerned, the IE is consistently lower for the somewhat larger basis (TZV2D) by 2−3 kcal mol^{-1} for benzene and naphthalene.

There are little experimental data to compare with the computational predictions.[35] Thermal desorption experiments of polyaromatic hydrocarbons from graphite lead to binding energies of 11.5 ± 1.8 kcal mol^{-1} for benzene and an average value of 19.6 ± 2.0 kcal mol^{-1} for naphthalene using two different methods of analysis. These experimental values span those from the various DFT calculations that we and other workers have performed. We also note that recently excellent agreement between a number of DFT schemes and spin component-scaled (SCS) SAPT0 methods has been found for smaller dimer systems.[36]

The results of our PM6-DH2 calculations for a C1006 graphene sheet and those of other workers are also given in Table 1. We have quoted our values averaged over a number of structures that differ by less than about 1.5 kcal mol^{-1}. We find IE values of −11.8 kcal mol^{-1} for benzene on a C1006 graphene sheet, the corresponding value for naphthalene being −18.9 kcal mol^{-1}. These values are close to those of −11.4 and −18.3 kcal mol^{-1} for benzene and naphthalene, respectively, reported[26] for a C1006 graphene sheet optimized at the molecular dynamics level. All these PM6-DH2 values are again within the error limits of the experimental measurements. For completeness, we have also used the PM6-D3 method, which is the PM6 method with Grimme's D3 correction for correlation,[37] to model benzene and naphthalene on a C574 graphene sheet. The corresponding values of −11.2 and −17.2 kcal mol^{-1}, respectively, are approximately 2 kcal mol^{-1} smaller than those from the PM6-DH2 method (Table 1), showing the very small effect of including H-bonding interactions. The value for naphthalene is now outside the experimental error boundary but only by 0.4 kcal mol^{-1}. We attribute the improved performance of PM6-DH2 to the reparameterization of the dispersive correction.[38] Our predicted IEs for pyrene and pentacene at the PM6-DH2 level, −29.4 and −41.0 kcal mol^{-1}, respectively, are in line with the finding of others that the strength of the interaction varies linearly with the number of carbons atoms. Thus, for the four aromatic hydrocarbons, we have considered having 6, 10, 16, and 22 carbon atoms, and the IE is between −1.8 and −2.0 kcal mol^{-1} for each carbon atom. From our comparison with higher level calculations, we thus consider that the PM6-DH2 method is of comparable accuracy to the more computationally demanding DFT methods and is to be somewhat preferred to the PM6-D3 scheme.

To further validate this approach, we have evaluated the IE of C_6F_6 with a C1006 graphene sheet yielding an average value of −16.4 kcal mol^{-1} for a number of configurations to be compared with values of −15.5 and −15.7 kcal mol^{-1} reported by Wang et al.[27] at the ωB97X-D/def2-TZVPP level for a $C_{110}H_{26}$ sheet. We have also studied the effect of ring substitution via calculations on 1,5-diaminonaphthalene, where again the IE is increased. Thus, our studies of benzene and naphthalene substitution show that the IE is increased irrespective as to whether the substituent is electron withdrawing or donating. A similar result has recent been reported by Bailey et al.[33] from their studies of pyrene- and anthracene-based families of adsorbates.

2.2. Adsorption of TCNE, TCNQ, and Derivatives of Pyrene Sulfonic Acids. The noncovalent functionalization of graphene has recently been reviewed by Mann and Dichtel,[40] and an experimental and computational study of the exfoliation mechanism of graphene with organic dyes has been described by Schlierf et al.[41] We now report our computations of the binding to graphene of some of the adsorbates reported in these two studies. The adsorption of electron acceptor molecules onto SLG, which is an electron donor, could modify its electronic properties. Thus, the adsorption of small p-type dopants such as tetracyanoethylene (TCNE), tetracyanoquinodimethane (TCNQ), and its perfluorinated derivative (F4-TCNQ) has been studied both experimentally[42] and computationally.[39,43,44] We note that although DFT studies using flexible basis sets can predict the degree of charge transfer upon adsorption, our semiempirical studies employing a minimal basis predict essentially no such charge transfer. However, our PM6-DH2 IE values are in line with those from DFT studies.[39] Thus, our DFT calculation of TCNQ (Table 1) yields an IE value close to the PM6-DH2 value. We also find (Table 1) that both TCNQ and F4-TCNQ have considerably greater IE values than TCNE, in line with their larger π-electron system, with fluorination increasing the IE as was found for benzene. Indeed the difference in the values for TCNE and TCNQ (12 kcal mol^{-1}) is close to the value for benzene itself. In their studies of the binding of TCNE and TCNQ, using dispersion augmented DFT methods, Hobza et al.[39] find that the IE values are significantly dependent upon the method employed, with our semiempirical values being quite close to their DFTB-D values, although they suggest that the BLYP-D3 values are closer to benchmark studies on smaller systems.

A number of pyrene sulfonic acid sodium salts have been studied experimentally to assess their efficacy as surfactants for graphene liquid phase exfoliation.[41] The four molecules studied, PS1, PS2, PS3, and PS4 (Figure 1), have groups (−SO_3^-, −OH) chosen for their properties such as water solubility, lack of toxicity, and well-defined adsorption and emission spectra. All four molecules were found to be adsorbed onto graphene and to be effective for graphene solubilization. We found that at the PM6-DH2 level it was not possible to obtain an optimal structure for these species adsorbed onto graphene because dissociation of the adsobate occurred. However, when the system was embedded in a dielectric continuum using the COSMO scheme, to model solvation in water, stable adsorbate-

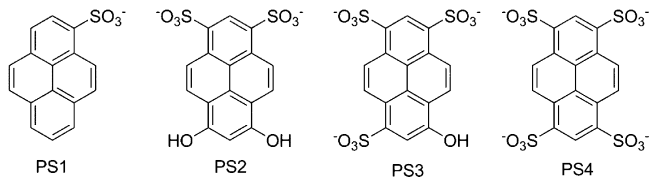

Figure 1. Chemical formula of pyrene derivatives.

dx.doi.org/10.1021/ci5003729 | J. Chem. Inf. Model. 2014, 54, 2255−2260

graphene structures were obtained. We can attribute this to the stabilization of the highly charged species by the dielectric continuum. IE values for these optimal structures, but without the continuum, were then evaluated to give the "gas phase" interaction energies shown in Table 2. We see that although the interaction energy of PS1 is less than that of pyrene itself, the IE increases rapidly as the overall negative charge increases. However, it is to be expected that these values will be greatly affected by solvation effects that we now consider for all the systems studied.

Table 2. Solvation and Interaction Energies in Water (kcal mol^{-1}) of Pyrene Sulfonic Acids[a]

species	solvation energy	interaction energy
PS1: $PyrSO_3H_3^{-1}$	−81.0	−21.3 [−12.8] (−19.9)
PS2: $Pyr(SO_3)_2(OH)_2^{-2}$	−214.8	−16.8 [−14.6] (−49.0)
PS3: $Pyr(SO_3)_3OH^{-3}$	−341.3	−13.0 [−11.8] (−67.8)
PS4: $Pyr(SO_3)_3^{-4}$	−518.0	−9.3 [−8.4] (−122.0)

[a]Gas phase values are in parentheses. Adsorption free energies from ref 41 are in square brackets.

3. SOLVATION EFFECTS

We have taken the "gas phase" structures optimized at the PM6-DH2 level (excluding PS1−PS4, Table 2) and included the effect of solvent using the COSMO continuum scheme as implemented in the MOPAC code. Our "gas phase" IE values do not include zero point or thermodynamic or entropic effects, so their correction with solvation-free energies does not yield a true free energy of binding. An alternative approach to the use of implicit solvent is to estimate the free energy of binding in the presence of explicit water molecules by the use of the potential of mean force (PMF) method employing an appropriate force field. This has been carried out by Hobza et al.[39] for TCNE and TCNQ and for PS1−PS4 by Schlierf et al.[41] Although no experimental data exist to assess the accuracy of our COSMO calculations, we can compare these two alternative approaches for a limited number of cases. We first note that the predicted free energy of solvation of benzene itself is predicted to be −2.0 kcal mol^{-1}, in good agreement both with the experimental value of −0.8 kcal mol^{-1}[45] and with free energy perturbation (FEP) and the inhomogeneous fluid solvation theory (IFST).[46] As in the case of gas phase adsorption, we report (Table 3) IE values for a number of adsorbates (Table 1) averaged over a number of configurations that are close in energy.

For all the substrates we have studied, adsorption upon the graphene sheet reduces the IE from its gas phase value due to the partial desolvation of the substrate upon binding to the graphene. For adsorption of three of the aromatic hydrocarbons we have studied, we find that the effect of solvation on the IE is quite small, reducing their magnitude by ∼1, 1, and 4 kcal mol^{-1} for benzene, naphthalene, and pentacene, respectively, in line with the corresponding predicted solvation energies of −2.0, −3.3, and −6.7 kcal mol^{-1} for the hydrocarbons. For these hydrocarbons, as well as for the other adsorbates, the IE in aqueous solution is reduced from the gas phase value by approximately half of the adsorbate solvation energy. This is as expected because solvation of one face of the adsorbate is lost upon binding to the graphene sheet. Thus, for example, in the case of diaminonaphthalene, the reduction in the IE value upon solvation is greater than for the unsubstituted hydrocarbon (∼6 compared to 1 kcal mol^{-1}) due to the greater solvation energy (−11.7 kcal mol^{-1}) of the substituted naphthalene. We find a similar situation for TCNE and TCNQ, having solvation energies of −10.9 and −15.5 kcal mol^{-1}, respectively, where the IE value is reduced by 4−5 kcal mol^{-1} upon solvation. These reductions are close to those reported by Hobza et al. for PMF studies, although their value for TCNQ is rather larger than ours (∼10 kcal mol^{-1}).

Table 3. Average Solvation and Interaction Energies (kcal mol^{-1}) in Gas Phase and Aqueous Solution for a Number of Adsorbates[a]

adsorbate	solvation energy	IE (gas phase)	IE (solution)	ΔIE (solvation)
benzene	−2.0	−11.8	−10.9	0.9
pentacene	−6.7	−41.0	−37.2	3.8
TCNQ	−15.5	−27.2	−21.9	5.4
tetrafluoro TCNQ	−13.0	−29.9	−24.2	5.7
TCNE	−10.9	−15.2	−11.3	3.8
naphthalene	−3.3	−18.9	−17.5	1.4
1,5-diaminonaphthalene	−11.7	−24.1	−18.2	5.9
pyrene	−4.8	−29.4	−26.7	2.6

[a]Reduction in the IE value (ΔIE) upon solvation is also given.

The sulfonated pyrenes are especially interesting because experimental data have been reported for these species. For these ionic species, solvation effects are as expected particularly important. The gas phase IE values are increasingly modulated by solvation as the ionic charge increases, and solvation energy is lost upon binding to the graphene sheet. It is due to this loss that the increase in the gas phase IE, found with increasing ionic charge, is reversed in aqueous solution, leading to an actual decrease in IE with increasing negative charge. The adsorption free energies for these four species have been computed by Schlierf et al.[41] using a PMF/MM scheme; a comparison with our values is shown in Table 2.

We find surprisingly close agreement between these two approaches except for the significantly smaller value found by Schierf et al.[41] for PS1. Thus, while all of our IE values decrease with increasing negative charge, Schierf et al. find that the adsorption free energy of PS2 is greater than that of the other three molecules. Experimentally, it is found that "the concentration of graphene exfoliated and dissolved from bulk graphite to suspension is highest for the PS2 derivative....The adsorption of the molecules from solution to bulk graphite is simply inversely proportional to the number of highly polar sulfonic groups present". Clearly the calculations of Schierf et al. correlate with the former observation, while our results correlate with the latter.

4. CONCLUSIONS

The objective of the present study has been to establish a robust yet computationally accurate scheme for predicting the adsorption energies of a range of unsaturated molecules that are relevant to the functionalization of graphene and to the exfoliation graphene sheets from graphite. It has been shown by a number of groups that dispersive interactions are crucial to modeling these interactions and that an economic yet accurate way of describing them is to augment an appropriate quantum mechanical model based upon either DFT or the semiempirical MO theory with an empiric pairwise interaction term. In Table 1, we show the corrections to the interaction energies that are

not present in the basic PM6 method. Our results again show that the dispersive corrections are the dominant contribution to the intermolecular interaction and that the PM6 scheme modified in this way (PM6-DH2) can be used to predict accurate adsorption energies of a variety of molecules on large graphene sheets to an accuracy comparable to both the limited experimental data currently available and to that achieved by higher level quantum mechanical methods. For the aromatic hydrocarbons, the effect of increasing their IE upon their substitution by both electron-donating and -withdrawing groups identified by DFT calculations has been shown to be quantitatively predicted by the PM6-DH2 method. It is of interest to note that the corresponding reduction of the IE in solution depends upon the magnitude of the solvation energy of the adsorbate, so that the effect of substitution on the IE is reduced in aqueous solution. Thus, for example, the IE of diaminonaphthalene is increased from that of naphthalene by ~5 kcal mol^{-1} in the gas phase but is predicted to be only 1 kcal mol^{-1} greater in aqueous solution, a quantity within the limits of accuracy of our calculations (Table 3).

Although there have been several DFT studies of the interaction of the smaller aromatic hydrocarbons with graphene providing the necessary benchmarks for semiempirical studies, there are only limited studies for the adsorption of more complex molecules. For example, a thorough study of TCNE and TCNQ on graphene-like molecules using DFT methods gave IE values that varied by up to 8 kcal mol^{-1}, although benchmark studies on smaller systems were valuable in reducing this uncertainty.

For these calculations to be of value to experimentalists, the inclusion of solvation effects is essential. The use of continuum models is the more straightforward and computationally efficient way of achieving this. In the absence of quantitative experimental data of the adsorption energies in solution, we have compared our COSMO calculations with PMF studies of TCNE, TCNQ, and PS1−PS4 adsorbates. We generally find good agreement, except for the values for PS1 where further studies are required.

AUTHOR INFORMATION

Corresponding Author

*E-mail: Ian.hillier@manchester.ac.uk.

Notes

The authors declare no competing financial interest.

REFERENCES

(1) Novoselov, K. S.; Geim, A. K.; Morozov, S. V.; Jiang, D.; Zhang, Y.; Dubonos, S. V.; Grigorieva, I. V.; Firsov, A. A. Electric field effect in atomically thin carbon films. *Science* **2004**, *306*, 666−669.

(2) Novoselov, K. S.; Geim, A. K.; Morozov, S. V.; Jiang, D.; Katsnelson, M. I.; Grigorieva, I. V.; Dubonos, S. V.; Firsov, A. A. Two-dimensional gas of massless Dirac fermions in graphene. *Nature* **2005**, *438*, 197−200.

(3) Tian, X. Q.; Xu, J. B.; Wang, X. M. Band gap opening of bilayer graphene by F4-TCNQ molecular doping and externally applied electric field. *J. Phys. Chem. B* **2010**, *114*, 11377−11381.

(4) Geim, A. K.; Novoselov, K. S. The rise of graphene. *Nat. Mater.* **2007**, *6*, 183−191.

(5) Hernandez, Y.; Nicolosi, V.; Lotya, M.; Blighe, F. M.; Sun, Z. Y.; De, S.; McGovern, I. T.; Holland, B.; Byrne, M.; Gun'ko, Y. K.; Boland, J. J.; Niraj, P.; Duesberg, G.; Krishnamurthy, S.; Goodhue, R.; Hutchison, J.; Scardaci, V.; Ferrari, A. C.; Coleman, J. N. High-yield production of graphene by liquid-phase exfoliation of graphite. *Nat. Nanotechnol* **2008**, *3*, 563−568.

(6) Lotya, M.; Hernandez, Y.; King, P. J.; Smith, R. J.; Nicolosi, V.; Karlsson, L. S.; Blighe, F. M.; De, S.; Wang, Z. M.; McGovern, I. T.; Duesberg, G. S.; Coleman, J. N. Liquid phase production of graphene by exfoliation of graphite in surfactant/water solutions. *J. Am. Chem. Soc.* **2009**, *131*, 3611−3620.

(7) Guardia, L.; Fernandez-Merino, M. J.; Paredes, J. I.; Solis-Fernandez, P.; Villar-Rodil, S.; Martinez-Alonso, A.; Tascon, J. M. D. High-throughput production of pristine graphene in an aqueous dispersion assisted by non-ionic surfactants. *Carbon* **2011**, *49*, 1653−1662.

(8) Smith, R. J.; Lotya, M.; Coleman, J. N. The importance of repulsive potential barriers for the dispersion of graphene using surfactants. *New J. Phys.* **2010**, *12*, 125008.

(9) Wang, Q. H.; Hersam, M. C. Room-temperature molecular-resolution characterization of self-assembled organic monolayers on epitaxial graphene. *Nat. Chem.* **2009**, *1*, 206−211.

(10) Jurecka, P.; Sponer, J.; Cerny, J.; Hobza, P. Benchmark database of accurate (MP2 and CCSD(T) complete basis set limit) interaction energies of small model complexes, DNA base pairs, and amino acid pairs. *Phys. Chem. Chem. Phys.* **2006**, *8*, 1985−1993.

(11) McNamara, J. P.; Sharma, R.; Vincent, M. A.; Hillier, I. H.; Morgado, C. A. The non-covalent functionalisation of carbon nanotubes studied by density functional and semi-empirical molecular orbital methods including dispersion corrections. *Phys. Chem. Chem. Phys.* **2008**, *10*, 128−135.

(12) Sato, T.; Tsuneda, T.; Hirao, K. Long-range corrected density functional study on weakly bound systems: Balanced descriptions of various types of molecular interactions. *J. Chem. Phys.* **2007**, *126*, 234114.

(13) Wu, Q.; Yang, W. T. Empirical correction to density functional theory for van der Waals interactions. *J. Chem. Phys.* **2002**, *116*, 515−524.

(14) Johnson, E. R.; Becke, A. D. A post-Hartree-Fock model of intermolecular interactions. *J. Chem. Phys.* **2005**, *123*, 024101.

(15) Johnson, E. R.; Becke, A. D. A post-Hartree-Fock model of intermolecular interactions: Inclusion of higher-order corrections. *J. Chem. Phys.* **2006**, *124*, 174104.

(16) Wu, X.; Vargas, M. C.; Nayak, S.; Lotrich, V.; Scoles, G. Towards extending the applicability of density functional theory to weakly bound systems. *J. Chem. Phys.* **2001**, *115*, 8748−8757.

(17) Jurecka, P.; Cerny, J.; Hobza, P.; Salahub, D. R. Density functional theory augmented with an empirical dispersion term. Interaction energies and geometries of 80 noncovalent complexes compared with ab initio quantum mechanics calculations. *J. Comput. Chem.* **2007**, *28*, 555−569.

(18) Grimme, S. Accurate description of van der Waals complexes by density functional theory including empirical corrections. *J. Comput. Chem.* **2004**, *25*, 1463−1473.

(19) Morgado, C.; Vincent, M. A.; Hillier, I. H.; Shan, X. Can the DFT-D method describe the full range of noncovalent interactions found in large biomolecules? *Phys. Chem. Chem. Phys.* **2007**, *9*, 448−451.

(20) McNamara, J. P.; Hillier, I. H. Semi-empirical molecular orbital methods including dispersion corrections for the accurate prediction of the full range of intermolecular interactions in biomolecules. *Phys. Chem. Chem. Phys.* **2007**, *9*, 2362−2370.

(21) Stewart, J. P. Application of the PM6 method to modeling proteins. *J. Mol. Model.* **2009**, *15*, 765−805.

(22) Rezac, J.; Fanfrlik, J.; Salahub, D.; Hobza, P. Semiempirical quantum chemical pm6method augmented by dispersion and h-bonding correction terms reliably describes various types of non-covalent complexes. *J. Chem. Theory Comput.* **2009**, *5*, 1749−1760.

(23) Tuttle, T.; Thiel, W. OMχ-D: Semiempirical methods with orthogonalization and dispersion corrections. Implementation and biochemical application. *Phys. Chem. Chem. Phys.* **2008**, *10*, 2159−2166.

(24) Stewart, J. J. P. *MOPAC2012*; Stewart Computational Chemistry, Colorado Springs: CO, 2012.

(25) Stewart, J. J. P. Application of localized molecular orbitals to the solution of semiempirical self-consistent field equations. *Int. J. Quantum Chem.* **1996**, *58*, 133−146.
(26) Gordeev, E. G.; Polynski, M. V.; Ananikov, V. P. Fast and accurate computational modeling of adsorption on graphene: a dispersion interaction challenge. *Phys. Chem. Chem. Phys.* **2013**, *15*, 18815−18821.
(27) Wang, W.; Zhang, Y.; Wang, Y.-B. Noncovalent $\pi\cdots\pi$ interaction between graphene and aromatic molecule: Structure, energy, and nature. *J. Chem. Phys.* **2014**, *140*, 094302.
(28) Grimme, S. Semiempirical GGA-type density functional constructed with a long-range dispersion correction. *J. Comput. Chem.* **2006**, *27*, 1787−1799.
(29) Zhao, Y.; Truhlar, D. G. The M06 suite of density functionals for main group thermochemistry, thermochemical kinetics, noncovalent interactions, excited states, and transition elements: two new functionals and systematic testing of four M06-class functionals and 12 other functionals. *Theor. Chem. Acc.* **2008**, *120*, 215−241.
(30) Raju, R. K.; Ramraj, A.; Hillier, I. H.; Vincent, M. A.; Burton, N. A. Carbohydrate-aromatic pi interactions: a test of density functionals and the DFT-D method. *Phys. Chem. Chem. Phys.* **2009**, *11*, 3411−3416.
(31) Chai, J. D.; Head-Gordon, M. Long-range corrected hybrid density functionals with damped atom-atom dispersion corrections. *Phys. Chem. Chem. Phys.* **2008**, *10*, 6615−6620.
(32) Weigend, F.; Ahlrichs, R. Balanced basis sets of split valence, triple zeta valence and quadruple zeta valence quality for H to Rn: Design and assessment of accuracy. *Phys. Chem. Chem. Phys.* **2005**, *7*, 3297−3305.
(33) Bailey, S.; Visontai, D.; Lambert, C. J.; Bryce, M. R.; Frampton, H.; Chappell, D. A study of planar anchor groups for graphene-based single-molecule electronics. *J. Chem. Phys.* **2014**, *140*.
(34) Frisch, M. J.; Trucks, G. W.; Schlegel, H. B.; Scuseria, G. E.; Robb, M. A.; Cheeseman, J. R.; Scalmani, G.; Barone, V.; Mennucci, B.; Petersson, G. A.; Nakatsuji, H.; Caricato, M.; Li, X.; Hratchian, H. P.; Izmaylov, A. F.; Bloino, J.; Zheng, G.; Sonnenberg, J. L.; Hada, M.; Ehara, M.; Toyota, K.; Fukuda, R.; Hasegawa, J.; Ishida, M.; Nakajima, T.; Honda, Y.; Kitao, O.; Nakai, H.; Vreven, T.; Montgomery, J. A.; Peralta, J. E.; Ogliaro, F.; Bearpark, M.; Heyd, J. J.; Brothers, E.; Kudin, K. N.; Staroverov, V. N.; Kobayashi, R.; Normand, J.; Raghavachari, K.; Rendell, A.; Burant, J. C.; Iyengar, S. S.; Tomasi, J.; Cossi, M.; Rega, N.; Millam, J. M.; Klene, M.; Knox, J. E.; Cross, J. B.; Bakken, V.; Adamo, C.; Jaramillo, J.; Gomperts, R.; Stratmann, R. E.; Yazyev, O.; Austin, A. J.; Cammi, R.; Pomelli, C.; Ochterski, J. W.; Martin, R. L.; Morokuma, K.; Zakrzewski, V. G.; Voth, G. A.; Salvador, P.; Dannenberg, J. J.; Dapprich, S.; Daniels, A. D.; Farkas; Foresman, J. B.; Ortiz, J. V.; Cioslowski, J.; Fox, D. J. *Gaussian 09*, Revision B.01; Gaussian, Inc.: Wallingford, CT, 2009.
(35) Zacharia, R.; Ulbricht, H.; Hertel, T. Interlayer cohesive energy of graphite from thermal desorption of polyaromatic hydrocarbons. *Phys. Rev. B* **2004**, *69*, 155406.
(36) Li, A.; Muddana, H. S.; Gilson, M. K. Quantum mechanical calculation of noncovalent interactions: A large-scale evaluation of PMx, DFT, and SAPT approaches. *J. Chem. Theory Comput.* **2014**, *10*, 1563−1575.
(37) Grimme, S.; Antony, J.; Ehrlich, S.; Krieg, H. A consistent and accurate ab initio parametrization of density functional dispersion correction (DFT-D) for the 94 elements H-Pu. *J. Chem. Phys.* **2010**, *132*, 154104.
(38) Řezáč, J.; Fanfrlík, J. i.; Salahub, D.; Hobza, P. Semiempirical quantum chemical PM6 method augmented by dispersion and H-bonding correction terms reliably describes various types of noncovalent complexes. *J. Chem. Theory Comput.* **2009**, *5*, 1749−1760.
(39) Haldar, S.; Kolar, M.; Sedlak, R.; Hobza, P. Adsorption of organic electron acceptors on graphene-like molecules: Quantum chemical and molecular mechanical study. *J. Phys. Chem. C* **2012**, *116*, 25328−25336.
(40) Mann, J. A.; Dichtel, W. R. Noncovalent functionalization of graphene by molecular and polymeric adsorbates. *J. Phys. Chem. Lett.* **2013**, *4*, 2649−2657.
(41) Schlierf, A.; Yang, H. F.; Gebremedhn, E.; Treossi, E.; Ortolani, L.; Chen, L. P.; Minoia, A.; Morandi, V.; Samori, P.; Casiraghi, C.; Beljonne, D.; Palermo, V. Nanoscale insight into the exfoliation mechanism of graphene with organic dyes: Effect of charge, dipole and molecular structure. *Nanoscale* **2013**, *5*, 4205−4216.
(42) Chen, W.; Chen, S.; Qi, D. C.; Gao, X. Y.; Wee, A. T. S. Surface transfer p-type doping of epitaxial graphene. *J. Am. Chem. Soc.* **2007**, *129*, 10418−10422.
(43) Denis, P. A. Chemical reactivity of electron-doped and hole-doped graphene. *J. Phys. Chem. C* **2013**, *117*, 3895−3902.
(44) Wang, Y. X.; Xu, Z. F.; Moe, Y. N. On the performance of local density approximation in describing the adsorption of electron donating/accepting molecules on graphene. *Chem. Phys.* **2012**, *406*, 78−85.
(45) Bennaim, A.; Marcus, Y. Solvation thermodynamics of nonionic solutes. *J. Chem. Phys.* **1984**, *81*, 2016−2027.
(46) Huggins, D. J.; Payne, M. C. Assessing the accuracy of inhomogeneous fluid solvation theory in predicting hydration free energies of simple solutes. *J. Phys. Chem. B* **2013**, *117*, 8232−8244.